Orbital Specific Chirality and Homochiral Self-Assembly of Achiral Molecules Induced by Charge Transfer and Spontaneous Symmetry Breaking

A. Mugarza,[1] N. Lorente,[1] P. Ordejón,[1] C. Krull,[1] S. Stepanow,[1] M.-L. Bocquet,[2] J. Fraxedas,[1] G. Ceballos,[1] and P. Gambardella[1,3]

[1]*Centre d'Investigació en Nanociència i Nanotecnologia (ICN-CSIC), UAB Campus, E-08193 Bellaterra, Spain*
[2]*Laboratoire de Chimie, UMR 5532, Ecole Normale Supérieure, F-69007 Lyon, France*
[3]*Institució Catalana de Recerca i Estudis Avançats (ICREA), E-08100 Barcelona, Spain*

(Received 26 May 2009; revised manuscript received 16 July 2010; published 10 September 2010)

We study the electronic mechanisms underlying the induction and propagation of chirality in achiral molecules deposited on surfaces. Combined scanning tunneling microscopy and *ab initio* electronic structure calculations of Cu-phthalocyanines adsorbed on Ag(100) reveal the formation of chiral molecular orbitals in structurally undistorted molecules. This effect shows that chirality can be manifest exclusively at the electronic level due to asymmetric charge transfer between molecules and substrate. Single molecule chirality correlates with attractive van der Waals interactions, leading to the propagation of chirality at the supramolecular level. Ostwald ripening provides an efficient pathway for complete symmetry breaking and self-assembly of homochiral supramolecular layers.

DOI: 10.1103/PhysRevLett.105.115702 PACS numbers: 64.75.Yz, 68.37.Ef, 68.43.−h, 81.16.Dn

Chirality plays a fundamental role in molecular recognition processes, providing selectivity to many life-regulating chemical reactions. Chiral molecules exist in two nonsuperposable mirror-image forms, called enantiomers, that display dramatically different activity in important classes of compounds such as pharmaceuticals and crop-protection chemicals [1]. To improve the production of enantiomerically pure compounds, chirally modified metal surfaces have been intensively studied in the last two decades as heterogeneous catalysts [2,3]. Recently, chiral surfaces have assumed central importance to a diverse range of investigations, including the amplification of nonlinear optical properties [4] and the asymmetric scattering of spin-polarized electrons [5,6]. Common to these fields, is the problem of how to confer chiral properties to otherwise achiral metal substrates.

A particularly efficient way of bestowing chirality to surfaces relies on the deposition of organic molecular films [7,8]. In such systems, chirality can be expressed at different levels: local (single molecule) [9], organizational (supramolecular) [10,11], or both [2,12]. It is well known that the adsorption of chiral molecules leads to the expression of both types of chirality. However, naturally occurring *achiral* molecules may also become chiral upon deposition on single-crystal surfaces, adding handedness to a vast library of chemical functions. This has been observed for specific (prochiral) molecular geometries owing to confinement in two dimensions [13,14] as well as molecules that undergo conformational changes upon adsorption [15,16]. Highly symmetric molecules locked to a substrate with dissimilar point-group symmetry have also been shown to develop chiral ordering through asymmetric intermolecular interactions [17,18]. Although a significant effort has been directed towards the structural characterization of adsorbed molecules and supramolecular domains in relation to chirality, little is known about their electronic properties and substrate-molecule interactions that ultimately lead to chirally modified surfaces.

In this Letter, we address the mechanisms of chiral induction and propagation of achiral molecules deposited on a metallic substrate. We present the case of square-planar Cu-phthalocyanines (CuPc) adsorbed on Ag(100) as a model system where the individual symmetry of adsorbate and substrate does not necessarily lead to chirality. Scanning tunneling microscopy (STM) measurements and density functional theory (DFT) calculations reveal the formation of chiral molecular orbitals in a structurally undistorted molecule, showing that substrate-induced enantiomerism can be of purely electronic nature and escape structural investigations. Attractive intermolecular interactions lead to the formation of supramolecular clusters with organizational chirality correlated to the handedness of the individual molecules. We further show that spontaneous symmetry breaking occurs thanks to the amplification of small inequalities in the initial distribution of supramolecular enantiomers and reversible single molecule chirality, leading to the self-assembly of electronically and structurally enantiopure layers over mesoscopic dimensions.

Figure 1(a) shows the adsorption geometry of CuPc monomers on Ag(100), deposited in ultrahigh vacuum by organic molecular beam epitaxy with the sample at room temperature. STM measurements were carried out *in situ* at 5 K. Similarly to previous investigations on low-index metal surfaces [19,20], CuPc molecules adsorb parallel to the substrate plane. We observe two different azimuthal orientations corresponding to molecules rotated by $\pm 30°$ ($\pm 2°$) relative to the [011] surface direction, with the

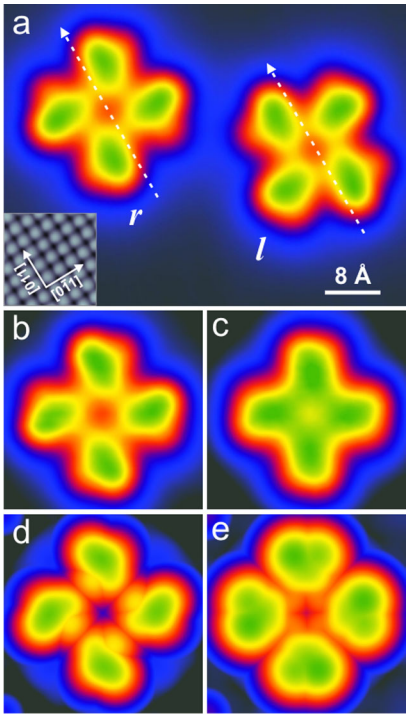

FIG. 1 (color online). STM images of CuPc adsorbed on Ag(100). (a) Molecules rotated by $+/-30°$ with respect to the [011] crystallographic direction (inset) show r/l chirality at bias voltage $V_b = -0.3$ V. (b) STM image of r-CuPc obtained at $V_b = -1$ V and (c) $V_b = +0.3$ V compared to the corresponding (d) and (e) STM images calculated using DFT.

Cu ion on Ag hollow sites in both cases. STM images reveal strong and opposite chiral contrast for the two molecular orientations, denoted as r and l, respectively, which are mirror-symmetric with respect to the [011] axis. Enantiomorphism in a symmetry-matched molecule-substrate system represents a limiting case where point-group symmetry constraints alone cannot explain chiral induction [11,17,18]. Remarkably, chiral contrast in the STM images is strong at negative bias and progressively disappears at positive bias voltage, as shown in Figs. 1(b) and 1(c). This behavior suggests that chirality in this system is mainly of *electronic* origin, i.e., not related to the molecule conformation.

To unravel the complex electronic interactions that give rise to enantiomorphism in CuPc, we have performed an extensive set of *ab initio* calculations using the VASP implementation of DFT in the projected augmented plane wave scheme and the local density approximation (LDA) [22]. Results obtained with the generalized gradients (GGA) approximation differ only quantitatively, with LDA producing a stronger molecule-surface interaction that leads to a shorter adsorption distance and larger charge transfer. The calculated slab included 5 Ag atomic layers intercalated by 8 vacuum layers, and a 7×7 lateral supercell, relaxed until forces were smaller than 0.04 eV/Å [23]. In agreement with STM, we find that the preferred location of the Cu ion is the Ag hollow site, with a 0.14 eV energy gain over the next stable configuration. With respect to top sites, the Cu-surface distance decreases from 2.7 to 2.4 Å, leading to larger charge transfer from the substrate and stronger stabilization of the molecule. The minimum-energy azimuthal orientation corresponds to a 32° deviation of the Cu-ligand axis from the [011] direction of the surface. The driving force underlying such a rotation is the N-Ag bond that forms between the sp^2 orbitals localized on the *aza*-N atoms and the nearest Ag atoms of the top layer. In order to minimize the N-Ag distance, the molecule rotates as shown in Figs. 2(a) and 2(b).

The optimized CuPc configuration shows a remarkable net transfer of 0.85 electrons into the molecule, obtained using the Bader charge analysis [24], distributed mainly into the doubly-degenerate lowest unoccupied molecular orbital (LUMO) and, to a lesser extent, into the unoccupied counterpart of the singly occupied molecular orbital (SOMO). This is reflected in the projected density of states (PDOS) shown in Fig. 2(c), where both LUMO and minority spin SOMO resonances partially cross the Fermi level, shifting down by about 0.5 and 0.2 eV, respectively, with respect to LDA calculations of gas-phase CuPc [25]. The differential charge density of the CuPc/Ag(100) complex relative to CuPc and Ag(100) is reported in Figs. 2(a) and 2(b). The excess charge partly localizes on the Cu atom, as expected from the SOMO downshift, and, more importantly, on the N atoms and benzyne groups, reproducing the charge contour of the frontier orbitals [25]. Specifically, as the sp^2 states of the *aza*-N atoms have considerable weight in the LUMO, charge transfer largely involves the N-Ag bonds. These results show that the

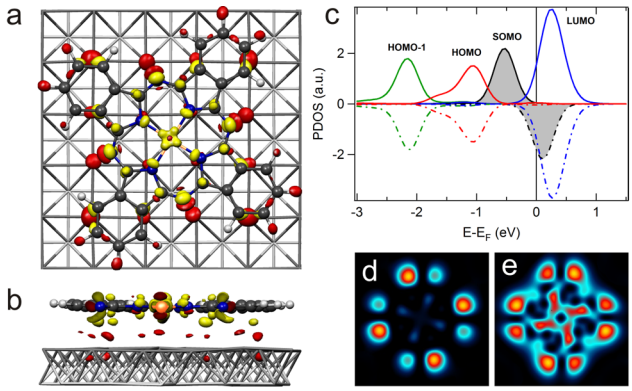

FIG. 2 (color online). (a) Top- and (b) diagonal side view of the differential charge density induced by molecular bonding to the substrate. The contour value is $\pm 3.8 \times 10^{-3}$ e/Å^3. The excess (depletion) of charge is shown in yellow (red). (c) Calculated DOS of r-CuPc/Ag(100) projected onto the unperturbed CuPc molecular orbitals. Positive (negative) units refer to spin up (down) states; a Gaussian broadening of 0.25 eV has been employed. (d),(e) Theoretical conductance maps at the peak position of the (d) HOMO and (e) LUMO.

adsorption of CuPc on Ag(100) implies a considerable degree of chemical bonding and that the molecular configuration is determined by N-specific interactions with the substrate. Importantly, the calculations disclose no significant distortion of the molecule, which remains planar as depicted in Fig. 2(b), showing no geometrical chirality due to adsorption.

The above findings explain the achiral topography of CuPc observed by STM at positive bias [Fig. 1(c)], and allow us to elucidate the electronic origin of chirality in the adsorbed molecules observed at negative bias [Figs. 1(a) and 1(b)]. The main source of chirality is the distortion of the highest occupied molecular orbital (HOMO) caused by direct interaction of the benzyne groups with the substrate atoms. This can be best observed by plotting the conductance maps obtained from the simulations at the HOMO/LUMO resonances [Figs. 2(d) and 2(e)], where the asymmetry between the two lobes located at the benzyne ring position is significantly more pronounced in the HOMO compared to the LUMO. Considering that the SOMO gives a negligible contribution to the tunneling current due to its d_{x^2-y2} character [20,21], the chiral contrast observed in the experimental and simulated STM images of Fig. 1, tuned to the HOMO/LUMO energy levels at -1.0 and 0.3 eV, respectively, reflect the different asymmetry of each orbital. The point chirality of CuPc molecules is therefore attributed to an electronic effect, which induces orbital-selective enantiomorphism of the molecular electron states in a well-defined energy range near the Fermi level.

A key question then is whether the chirality of the CuPc electron states can be transferred to extended two-dimensional layers. Chirality in adsorbed molecular arrays requires stereospecific molecular interactions, which are usually provided through either hydrogen bonds [13,14] or correlation of azimuthal molecular orientations with lateral van der Waals (VdW) forces [17,18]. Macrocyclic molecules such as phthalocyanines [19,20,26] and porphyrins [27,28] are known to assemble into ordered compact layers at surfaces, where spontaneous formation of organizational chiral domains occurs as a result of lattice-matching constraints and weak VdW attraction. In the absence of local enantiomorphism, however, the chirality expression is limited to the structure of the arrays. Further, there is no reason for one type of domain to prevail upon the other, and the coexistence of both type of organizational domains in the same molecular layer is observed [26–28]. The self-assembly of CuPc on Ag(100) significantly differs from such behavior, since the electronic chirality of each molecule is carried over to extended layers and correlated to organizational chirality. Moreover, spontaneous symmetry breaking occurs, leading to the formation of CuPc films with complete chiral purity over mesoscopic dimensions.

Figures 3(a) and 3(b) are representative of mirror-symmetric enantiopure CuPc domains. We observe single handedness of the molecular arrangement for each enantiomer, with the two domains corresponding to commensurate superlattices with 5×5 periodicity, rotated by $\pm 37°$ with respect to the [011] direction. The superlattice chirality is designated as R (L) for the 5×5 $R-(+)37°$ structure. The univocal relation between molecular and array chirality results in the preferential assembly of rR and lL domains, although a similar hollow site adsorption and CuPc close-packing fraction would be obtained for rL and lR configurations having 5×5 $R0°$ periodicity [23]. Figure 3(c) shows that this chiral propagation process is already active between isolated CuPc enantiomers, as the relative abundance of rR/rL, and lL/lR dimers in the earliest stages of aggregation is strongly asymmetric. To understand the mechanism of chiral recognition, we carried out calculations of both lL and lR phases (rR and rL being equivalent by symmetry) using SIESTA [29], and a new DFT functional explicitly designed to include VdW interactions [30,31]. The calculations show that the orientation of CuPc with respect to the substrate is the same for the two phases, so the structure of the monolayer is mainly determined by the CuPc-Ag interaction. However, the distances between adjacent phenyl groups in the lL phase are slightly smaller compared to lR, leading to a stabilization of the former due to attractive VdW interactions. The total energy difference between the two phases is of the order of 40 meV, which is reduced below the relative accuracy of the calculations (~10 meV) by removing the nonlocal VdW correlation [23]. We note that substrate-mediated enantiospecific interactions [32] may also lead to chiral recognition. Indeed, we find that the charge transfer between Ag and CuPc induces chiral asymmetry to the

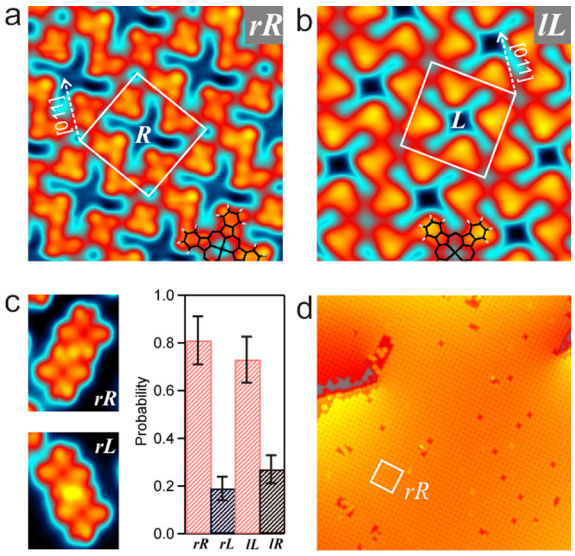

FIG. 3 (color online). Chiral self-assembly of CuPc. (a) rR and (b) lL homochiral domains recorded with $V_b = +0.52$ V and -0.10 V respectively. (c) rR and rL dimers shown together with the relative probability of each configuration (d) Homochiral rR domain extending over a terrace and crossing a screw dislocation. Image size 77.3×77.3 nm.

substrate metal states in the proximity of each molecule, but the resulting electrostatic potential energy difference between the *lL* and *lR* dimer configurations cancels out after integration over the whole area occupied by neighbor molecules [23].

Our data show that a racemic mixture of *rR* and *lL* domains is present on each terrace in the initial stages of growth (Fig. S4 in Ref. [23]), consistently with the fact that they are energetically equivalent. As the CuPc coverage approaches one monolayer; however, we observe that the symmetric population spontaneously breaks into a single homochiral phase, the extension of which is limited only by substrate steps [Fig. 3(d)]. This phenomenon is quite unusual since spontaneous organizational chiral resolution is not reported for similar systems [26–28]. Even for crystallization reactions in solution, achieving complete chiral purity is very rare when both enantiomers are present since the beginning [33]. However, mechanisms that enhance any initial imbalance in chirality and catalyze the production of one enantiomer while suppressing its mirror-image are important as they provide clues to spontaneous chiral symmetry breaking in nature. In the present case, chiral resolution occurs through two-dimensional Ostwald ripening, which allows for the exchange of molecules between supramolecular clusters of opposite handedness during the nucleation and growth process at room temperature [23]. Note that complete chiral purity can be reached only because both *rR* and *lL* domains can independently feed the growth of the majority phase. This is due to the intrinsic achiral nature of the molecules, which allows for switching of the surface-induced point-group chirality during molecular diffusion.

In conclusion, we have shown that surface-induced chirality can arise as a purely electronic effect irrespective of point-group symmetry arguments and propagate at the organizational level through chiral recognition and spontaneous symmetry breaking. STM and DFT calculations reveal that CuPc adsorbed on Ag(100) display orbital-specific electronic chirality caused by molecule-substrate asymmetric charge transfer, while the molecular conformation remains achiral. The electronic chirality of individual molecules is retained in extended layers and univocally transferred at the organizational level through lateral VdW interactions. With increasing molecular density, an equal mixture of supramolecular domains of opposite handedness evolves into mesoscopic homochiral CuPc layers due to spontaneous chiral symmetry breaking during self-assembly. The ability to grow enantiopure supramolecular layers and tune the chirality of distinct molecular orbitals may lead to novel ways to control the electronic properties and optical response of metal surfaces.

We acknowledge financial support from the Spanish Ministerio de Ciencia e Innovación (FIS2006-12117-C04-01, FIS2009-12721-C04-01 and MAT2007-62341) and the European Research Council (StG 203239). N. L. also thanks the Agence Nationale de la Recherche (JCJC06-148337) for partial funding, the Centre de Calcul Midi-Pyrénnées, and the Barcelona Supercomputing Center.

[1] H.-J. Federsel, Nat. Rev. Drug Discov. **4**, 685 (2005).
[2] M. O. Lorenzo *et al.*, Nature (London) **404**, 376 (2000).
[3] G. J. Hutchings, Annu. Rev. Mater. Res. **35**, 143 (2005).
[4] T. Verbiest *et al.*, Science **282**, 913 (1998).
[5] R. A. Rosenberg, M. A. Abu Haija, and P. J. Ryan, Phys. Rev. Lett. **101**, 178301 (2008).
[6] K. Ray *et al.*, Science **283**, 814 (1999).
[7] S. M. Barlow and R. Raval, Surf. Sci. Rep. **50**, 201 (2003).
[8] K.-H. Ernst, Top. Curr. Chem. **265**, 209 (2006).
[9] G. P. Lopinski *et al.*, Nature (London) **392**, 909 (1998).
[10] F. Charra and J. Cousty, Phys. Rev. Lett. **80**, 1682 (1998).
[11] M. Parschau *et al.*, Angew. Chem., Int. Ed. **46**, 8258 (2007).
[12] R. Fasel, M. Parschau, and K.-H. Ernst, Nature (London) **439**, 449 (2006).
[13] M. Böhringer *et al.*, Phys. Rev. Lett. **83**, 324 (1999).
[14] J. Weckesser *et al.*, Phys. Rev. Lett. **87**, 096101 (2001).
[15] Q. Chen, D. Frankel, and N. Richardson, Surf. Sci. **497**, 37 (2002).
[16] S. Weigelt *et al.*, Nature Mater. **5**, 112 (2006).
[17] M. Schock *et al.*, J. Phys. Chem. B **110**, 12835 (2006).
[18] N. V. Richardson, New J. Phys. **9**, 395 (2007).
[19] P. H. Lippel *et al.*, Phys. Rev. Lett. **62**, 171 (1989).
[20] X. Lu *et al.*, J. Am. Chem. Soc. **118**, 7197 (1996).
[21] S. Stepanow, A. Mugarza, G. Ceballos, P. Moras, J. C. Cezar, C. Carbone, and P. Gambardella, Phys. Rev. B **82**, 014405 (2010)
[22] G. Kresse and D. Joubert, Phys. Rev. B **59**, 1758 (1999).
[23] See supplementary material at http://link.aps.org/supplemental/10.1103/PhysRevLett.105.115702.
[24] R. F. W. Bader, W. H. Henneker, and P. E. Cade, J. Chem. Phys. **46**, 3341 (1967).
[25] A. Calzolari, A. Ferretti, and M. B. Nardelli, Nanotechnology **18**, 424013 (2007).
[26] Z. H. Cheng *et al.*, J. Phys. Chem. C **111**, 2656 (2007).
[27] W. Auwärter *et al.*, J. Chem. Phys. **124**, 194708 (2006).
[28] D. Ecija *et al.*, J. Phys. Chem. C **112**, 8988 (2008).
[29] J. M. Soler *et al.*, J. Phys. Condens. Matter **14**, 2745 (2002).
[30] G. Román-Peréz and J. M. Soler, Phys. Rev. Lett. **103**, 096102 (2009).
[31] M. Dion, H. Rydberg, E. Schröder, D. C. Langreth, and B. I. Lundqvist, Phys. Rev. Lett. **92**, 246401 (2004).
[32] S. Blankenburg and W. G. Schmidt, Phys. Rev. Lett. **99**, 196107 (2007).
[33] C. Viedma, Phys. Rev. Lett. **94**, 065504 (2005).